Radio-selected Galaxies in Very Rich Clusters at $z \leq 0.25$: II. Radio Properties and Analysis

Glenn E. Morrison
California Institute of Technology, IPAC, M/S 100-22, Pasadena, CA 91125; morrison@ipac.caltech.edu

Frazer N. Owen
National Radio Astronomy Observatory[1]*, P. O. Box O, Socorro, NM 87801; fowen@aoc.nrao.edu*

ABSTRACT

We report on the properties of radio-selected galaxies within 30 very-rich Abell clusters with $z \lesssim 0.25$. The radio, optical, and x-ray data for these clusters were presented in Paper I (Morrison et al. 2002). These radio data sample the ultra-faint ($L_{1.4} \geq 2 \times 10^{22}$ W Hz^{-1}) radio galaxy population with $M_{\rm R} \leq -21$ using the well-known FIR/radio correlation to link the radio with ongoing star formation within individual cluster galaxies. Spectroscopic redshifts exist for $\sim$96% of the optical identifications. These radio-selected galaxies reveal the 'active' galaxy population (starburst and active galactic nuclei) within these rich cluster environments that can be identified regardless of their level of dust obscuration. These new radio data provide the largest sample to date of low-luminosity radio galaxies within rich cluster environments allowing an unbiased search for dusty starbursting galaxies. For all clusters in our sample, we are sensitive to star formation rates (M ≥ 5M$_\odot$) $\gtrsim 5\,$M$_\odot$yr^{-1}. We have found that the excess number of low-luminosity 'starburst' radio-selected galaxies (SBRG) found by Owen et al. (1999) in Abell 2125 is *not* indicative of other rich clusters in our sample. The average fraction of SBRG is $\langle f_{\rm SBRG} \rangle = 0.022 \pm 0.003$. The A2125 fraction is $f_{\rm SBRG} = 0.09 \pm 0.03$ which is significantly different from the sample average at a $>$99.99% confidence level. Both A1278 and A1689 are slightly different from the rest of the sample at $\sim$90% confidence level. The bimodal structure of both the x-ray brightness distribution and optical adaptively smoothed images of A1278 and A2125 suggests that ongoing cluster-cluster mergers may be enhancing this SBRG population. The A1689 excess low-luminosity (and high-luminosity) radio galaxy population may be due to interaction with the ICM. The mid-infrared ISOCAM results for A1689's radio galaxy population suggests that the radio emission for both low- and high-luminosity radio galaxies is AGN in origin except for one radio galaxy. There is a significant spatial distribution difference between the low and high-luminosity (HLRG) radio-selected populations. The SBRG have a core radius of 0.40 ± 0.08 Mpc which is $>3\times$ larger than the HLRG core radius. In addition, 48% of the SBRGs have colors that are bluer than a typical Sab galaxy compared to 4% for the HLRGs. The average absolute magnitude for the SBRG's is $\langle M_{\rm R} \rangle = -21.93 \pm 0.05$, while for the HLRG's it is $\langle M_{\rm R} \rangle = -22.33 \pm 0.07$, indicating that the SBRG are less optically luminous than their HLRG counterparts. The HLRGs seem to be a subclass of the cluster's massive red elliptical population, while the SBRGs have a projected radial distribution more like the blue spiral population. Our results indicate that most of the SBRGs are probably gas-rich disk galaxies undergoing $\gtrsim 5\,$M$_\odot$ yr^{-1} of star-formation.

Subject headings: galaxies: evolution — galaxies: clusters: Abell — galaxies: starburst — radio continuum: galaxies

1. Introduction

Hierarchical clustering models predict that clusters of galaxies are assembled by a continuous coalescence of subclusters (**?**, e.g.,)]whi76,evr90b,lac93,lac94,bal98a. The ongoing mass accretion yields artifacts in the form of cluster asymmetry and significant amounts of subclustering. The remnants of structure formation are visible in current epoch clusters as substructure and cluster-cluster merging events. Estimates of detectable substructure in rich nearby clusters range from 30%-40% (**?**, e.g.,)]gel82, wes90. The timescale for the accretion events is ~ 1 Gyr for group-cluster encounters and ~ 4 Gyr for cluster-cluster mergers(Evrard 1990), compared to $\lesssim$0.3 Gyr for a typical starburst (SB)(**?**, e.g.,)]ken98. Such SB episodes show up as a cluster-wide enhancement of the radio-selected galaxy population. Therefore, while the substructure caused by large-scale-structure formation will be visible for a significant fraction of a Hubble time, the cluster-wide enhanced radio activity, as in the case of A2125 (Owen et al. 1999), will be rather brief.

The Butcher-Oemler (BO) effect (Butcher & Oemler 1984) has been suggested as a link between galaxy evolution and cluster dynamics. The hierarchical models predict that distant clusters assemble from smaller subclumps at a much higher rate than similar mass nearby clusters. These smaller groups have a higher fraction of gas-rich, late-type galaxies, thereby providing a distant cluster with a population that would support significant amounts of induced star formation (SF). In fact, these late-type galaxies may be transformed into early-type galaxies by environmental dynamics of the cluster (**?**, e.g.,)]oem97.

The Caldwell & Rose (1997) spectral study of early-type galaxies in rich clusters with significant substructure shows that $\sim 15\%$ of these galaxies have signatures of current or ongoing SF. This suggests that cluster-group merger activity signified by the substructure may alter the star formation rate (SFR) of a cluster galaxy population. Induced SF may result from shocks caused by the collision between the intracluster medium of the cluster and that of the group. Alternatively, the main driver of this activity may be galaxy-galaxy collisions in regions where the velocity dispersion is low enough and the density is high enough for such encounters to be efficient. The different regions that the starburst population inhabits within the rich cluster gives us clues as to the triggering mechanism for this activity. Radio observations allow us to identify this population without being hampered by dust extinction or the K-correction.

This paper is the second in a series studying the ultra-faint radio-selected galaxy populations associated with rich clusters of galaxies as a function of redshift. We analyze both the high and low luminosity radio-selected galaxy population within 30 very rich Abell clusters (richness $\geq$2) with $z \lesssim 0.25$. The data used in our analysis was presented in paper I (Morrison et al. 2002).

Initially, Dwarakanath & Owen (1999) conducted a VLA 20 cm wide-field continuum study of two very rich Abell clusters, A2125 and A2645, looking at the radio galaxy population down to $\sim 2\times10^{22}$ W Hz^{-1}. The reason for choosing this lower radio luminosity limit is that Condon et al. (1991) had determined that in the local universe this limit has a statistically higher fraction of starburst-powered radio-selected galaxies and few galaxies whose radio emission is powered by AGNs. Both clusters are at the same redshift (z=0.25) and richness (R=4), but A2125 has a higher blue galaxy population ($f_{\rm B}$ = 0.19) than A2645 ($f_{\rm B}$ = 0.03). The radio galaxy population is also substantially different: A2125 has 26 radio detected galaxies whereas A2645 has 4 (Owen et al. 1999).

Most of the radio galaxy population of A2125 is not confined to the core region of the cluster ($r <$ 400 kpc) but is distributed out to a radius of 2.5 Mpc. The radio-selected galaxies in the cluster core are red in color, with none of the blue Butcher-Oemler galaxies detected down to the radio luminosity limit. The origin for the radio emission is both AGN and massive ongoing SF. The latter occurs more frequently in the outer cluster region of A2125.

This result raises several interesting questions. Are we just seeing the infall of the field population at $z = 0.25$, or are we witnessing an enhancement in the activity level of the population due to the cluster environment? Do all very rich clusters show enhanced activity in the form of starburst

[1]The National Radio Astronomy Observatory is operated by Associated Universities, Inc., under a cooperative agreement with the National Science Foundation.

and AGNs, or only the ones at higher redshift?

To understand if this is a richness or a redshift effect, we have constructed a sample of 34 very rich clusters from $0.02 \lesssim z \lesssim 0.41$ to study how the radio properties of these clusters evolve (if at all) over the last ~5 Gyr. VLA radio observations at 20 cm offer a wide field-of-view (~30 arcmin), allowing us to sample out to 2.5 Mpc radius from the cluster core. Nearby clusters ($z \leq 0.06$) were analysed using the NRAO VLA Sky Survey (NVSS) which provided the required linear coverage (5 Mpc diameter search area) and sensitivity. At this projected distance from the cluster core we should detect any infalling starbursting field galaxies. Our detection limit of $2{\times}10^{22}$ W Hz^{-1} ($H_0 = 75\,\mathrm{km\,s^{-1}\,Mpc^{-1}}$; $q_0 = 0.1$) yields a SFR(M $\geq 5\mathrm{M}_\odot$) sensitivity limit of $\gtrsim 5$ M$_\odot$ yr^{-1} assuming the SFR relation from Condon (1992).

In this paper, we analyze the radio properties of 30 of the richest, nearest Abell clusters from $0.02 \lesssim$ z $\lesssim 0.25$. These clusters were chosen to be as rich or richer than the four $z = 0.4$ clusters. We investigate the characteristics of the different radio galaxy populations and their relationship to the cluster properties, such as richness, core richness, compactness, and x-ray luminosity. In addition, the Butcher-Oemler-defined blue color and absolute optical luminosity of the radio-selected objects are also explored.

2. The Radio-selected Galaxy Classes

In this study we were unable to spectroscopically classify radio-selected galaxies as starbursts or AGNs given the quality of the spectra. However, useful redshift measurements were obtained. The new spectroscopic data and resulting spectroscopic classifications of the radio-selected galaxies will be discussed in paper IV (Morrison et al. 2003b). Thus, we relied on statistical means to separate the galaxies into these two classes. Based on Figure 9 from Condon's con89 paper showing the local field galaxy radio luminosity function (RLF), we see that a luminosity of 10^{23} W Hz^{-1} divides the starburst-spiral population from the AGN-E/S0 population. Radio-selected galaxies with luminosities below this limit are statistically more likely to have their radio emission powered by non-thermal synchrotron emission as a by-product of massive SF. Table 1 defines the different radio luminosity classes. The different radio galaxy classes are high-luminosity (HLRG), low-luminosity (LLRG), and 'starburst' (SBRG). Most of the analysis will be concerned with the HLRG and the SBRG classes.

The SBRG class was created from the LLRG class because of the excess of early-type galaxies within galaxy clusters (Oemler 1974). As we can see in Condon's RLF plot, while the elliptical/AGN population drops below the starburst-spiral population at 10^{23} W Hz^{-1}, AGN powered radio galaxies below this break still exist. Given the larger population of early-type galaxies that inhabit clusters, we have chosen a lower break in the RLF at $10^{22.75}$ W Hz^{-1}. Based on the RLF, our SBRG should have a lower level of AGN contamination than the LLRG class. Therefore, statistically the SBRGs should be primarily powered by starbursts and the HLRGs by AGNs.

3. Spatial Distribution of Radio-selected Galaxies

The radial distribution with respect to the cluster center of the high- and low-luminosity radio galaxies allows us to examine how the different radio galaxy populations are distributed with respect to each other and the cluster environment. This may give us clues to their past history. Do low-luminosity radio-selected galaxies belong to some sort of subclass of the cluster population, *e.g.,* recently infalling star forming blue field galaxies or are they cluster blue galaxies?

3.1. Luminosity Class Spatial Distribution

We begin our examination with the spatial radial distribution of the radio-selected galaxies within the cluster (verified by spectroscopic redshift) as a function of projected distance from the cluster center. Our radio sample is complete out to a linear projected distance of 2.5 Mpc. Figure 1 shows the radio galaxy surface-density plotted against the projected distance from the center of the cluster. Thirty clusters were used. The centers are based on the X-ray center fits, with errors ± 15-25″ (Morrison et al. 2002). The surface density, $\sigma\,(\#/Mpc^2)$, was calculated by dividing the number of detections occurring in each bin by the annular search area in Mpc^2. The area of each annulus was multiplied by the number of surveyed clusters used to make the sample.

The distribution of the radio galaxies is rather striking. The high luminosity radio galaxies (HLRG) are very clustered near the cluster cores. This is consistent with the Ledlow & Owen (1995a,b) survey of 293 clusters, which showed that HLRGs (mostly FR I's) preferentially reside in the centers of rich clusters because the most optically luminous galaxies occur there.

The distribution of the SBRGs is a *new* result. Radio galaxies with luminosities between $10^{22.3-22.75}$ W Hz^{-1} seem to avoid the cluster centers and distribute themselves more widely (for $r < 1.0\,$Mpc), similar to blue galaxies in clusters. A Kolmogorov-Smirnov test between the spatial distributions of HLRGs and SBRGs indicates that they are from two separate parent populations at the $> 99\%$ confidence level. The SBRG's follow the more widely distributed cluster spiral population, while the HLRG's appear to trace the massive red E/S0 cluster population.

3.2. King Model Comparison

Clusters that are highly symmetric in projected shape and have a high concentration at the center or core are typically called "regular" and, in some cases, are believed to be virialized. These clusters are well-fit by the King model, represented by equation 1. This model is an analytical solution to the inner part of an isothermal function (King 1962):

$$\Sigma(r) = \frac{\Sigma_0}{1 + (r/r_\mathrm{c})^2}. \qquad (1)$$

Figure 2 shows an overabundance of high-luminosity radio galaxies near the cluster core, while figure 3 shows that the low-luminosity radio galaxies are more widely distributed than predicted, based on a virialized cluster. All radio-selected galaxies used in these plots have measured redshifts that are consistent with their cluster redshift. The dispersion or width measure seen in these plots is roughly defined by the core radius, r_c. The core radius is where the projected surface density is half the central density, Σ_0. The core radius is a function of cluster morphology (Sarazin & Quintana 1985), but several studies (Bahcall 1975; Girardi et al. 1995; Adami et al. 1998) have found values of r_c that are consistent with each other, yielding a value of ∼0.2 Mpc for regular clusters.

Assuming a King distribution for the radio galaxies, we determined the values of the core radii, r_c, that are compatible with the SBRGs and the HLRGs distributions. The integrated or cumulative King function,

$$\sigma(r) = \pi r_c^2 \ln(1 + (r/r_c)^2), \qquad (2)$$

which was normalized to one at r = 2.5 Mpc, was used with the K-S test to determine the r_c values for low- and high-luminosity radio-selected galaxy distribution. The results show that the SBRG population does not come from a King distribution with a small core ($r_c \sim 0.15\,$Mpc) radius that would fit the luminous radio population at a confidence level $> 99\%$.

The r_c derived values from a χ^2 fit to the King function for the different radio populations are $r_\mathrm{c} = 0.40 \pm 0.08$ Mpc and $r_\mathrm{c} = 0.12 \pm 0.02$ Mpc for the SBRGs and HLRGs, respectively. Morrison et al. (2003a) has found that $r_\mathrm{c} = 0.26 \pm 0.11\,$Mpc for the red population of regular clusters, which is similar to the r_c value for the HLRGs, suggesting that they are a subclass of a cluster's massive red population. Ledlow & Owen's led95a much larger sample shows this result much more strongly for the HLRGs. Morrison et al. (2003a) also found that the blue population for the compact clusters have $r_\mathrm{c} = 0.6 \pm 0.23\,$Mpc which is within the errors of the r_c value for SBRGs. Based on the SBRG radio luminosity and core radius value these galaxies seem to be a subclass of the cluster's blue galaxy population. Further evidence of this is given in section 4.1.1 and in figure 5ZZZ.

4. Radio Galaxy Fractions

The radio galaxy fraction of a cluster was defined in Paper I. Briefly, the fraction of radio galaxies, f_RG, is the number of radio galaxies normalized by the total number of galaxies, $N_{2.5}$, sampled (corrected for the background). $N_{2.5}$ is the number of galaxies within 2.5 Mpc of the cluster center with an absolute R magnitude cutoff of −21. The radio galaxy fraction for each cluster with n total galaxies is a binomial probability. We determined how this probability differs in a given cluster from a "true" probability derived from the sample as a whole. This imposes a constraint on the system reducing the degrees of freedom by one. From this method, we constructed 1σ errors for the f_{RG} values. Significant levels for clusters which have radio galaxy fractions inconsistent with the rest of the sample were calculated using the same method.

Table 1 shows the radio-selected galaxy classes we will study. Given the higher contamination of AGNs in the LLRG class we will analyze only the SBRG and HLRG populations. These two radio-selected populations will be investigated separately, in order to tell if any clusters show an excess fraction relative to the other rich clusters. If a large enhancement exists for a particular cluster, this will provide evidence that ongoing physical processes within the cluster environment may be causing these galaxies to have increased radio emission.

Given the uncertainty in the number of galaxies, $N_{2.5}$, within 2.5 Mpc of the cluster core and having $M_{\mathrm{R}} \leq -21$ for clusters with $z < 0.1$ (**?**, see)]mor00b, we will restrict our radio fraction analysis to clusters with $z > 0.1$.

4.1. The Radio-selected Population

We are now in a position to answer the following question: Is the radio galaxy population of A2125 ubiquitous for all rich clusters? Figure 4 shows the SBRG f_{RG} as a solid line for all $0.1 \lesssim z \lesssim 0.25$ clusters. A2125 has the largest fraction of SBRGs[2]; $f_{\mathrm{SBRG}} = 0.09 \pm 0.02$ which is significantly different from the rest of the sample at the $> 99.99\%$ confidence level. The mean for the SBRGs, $\langle f_{\mathrm{SBRG}} \rangle$, is 0.022 ± 0.003. Other clusters: A1278 and A1689 (both have $f_{\mathrm{SBRG}} = 0.05 \pm 0.03$) are different from the mean only at the $\sim 90\%$ confidence level. However, the large f_{RG}-value for A2125 is not a richness effect, since the total number of radio-selected objects has been normalized by the total number surveyed.

The spectroscopic classification of the radio-selected galaxies in A2125 is described in Owen et al. (1999). They find four classes of cluster radio galaxies (old stellar population (OSP), starbursts, AGN, and "intermediate") defined by their optical spectra[3] and colors. 50% (13/26) of these galaxies have spectral energy distributions (SED) similar to OSP, based on their colors and/or 4000Å break (D4000) and lack of emission lines. These 13 OSP galaxies have their radio luminosities divided into the following radio luminosity classes. SBRGs make up 31%, LLRGs 38%, and HLRGs 62%. All of the radio-selected galaxies classified as starbursts in the Owen et al. (1999) sample are SBRGs. The radio properties of their intermediate class, defined by their bluer colors and/or small D4000, but weak or undetected line emission, contain 88% SBRGs, 100% LLRGs, and no HLRGs. This suggests that these objects may have a young stellar component plus ongoing SF whose optical signature is hidden by dust. The only spectroscopically-confirmed AGN is an HLRG. Thus, 75% of the SBRGs appear to have active SF (62% for the LLRGs), while all the HLRGs appear to be AGN in nature.

The fraction of HLRGs in A2125 ($f_{\mathrm{RG}} = 0.03 \pm 0.01$) does not display any excess with respect to the other rich clusters in the sample as seen in Figure 4 where the HLRG radio galaxy fractions are represented by the hatched pattern. However, A1689 shows an enhanced f_{RG} value (0.10 ± 0.04) compared to the rest of the sample, which is significant at the $> 99.9\%$ level. A1940 has a slightly higher f_{HLRG} value than the rest of the sample at 0.06 ± 0.03 with a confidence level of 94%. The mean for the HLRGs is $\langle f_{\mathrm{RG}} \rangle = 0.024 \pm 0.003$.

4.1.1. Colors of Radio-selected Galaxies

In this section, we determine if a galaxy's optical color is dependent on its radio luminosity and also provide qualitative evidence for the probable power sources (AGN or starburst) for the radio emission.

After correcting for the color-magnitude (C-M) effect (*e.g.* Stanford et al. (1998)) and applying the K- correction to the radio-selected galaxy's color, we compare the $(B-R)_{\mathrm{RG}}$ color of the

[2] That is this cluster deviates from the rest of the sample by having an excess of galaxies in this range of radio luminosity.

[3] In the Owen et al. (1999) sample, characterization of the galaxies was done using the emission and absorption lines of the spectra.

galaxy to that of "blue galaxies" as defined by Butcher & Oemler (1984). BO defines blue galaxies as having rest-frame $B-V$ colors at least 0.2 magnitudes bluer ($\Delta\,(B-V)=0.2$)[4] than the E/S0 galaxy population. Details can be found in Morrison et al. (2003a). In brief, in the rest-frame for a particular galaxy, we calculated the average E/S0 color transformed to $B-R$, $\langle B-R\rangle_{(\mathrm{E/S0})}$, and the BO blue criterion, $\Delta\,(B-R)$. Radio-selected galaxies that obey

$$\langle B-R\rangle_{(\mathrm{E/S0})}-\Delta(B-R)\geq(B-R)_{\mathrm{RG}} \tag{3}$$

are defined as blue, where $(B-R)_{\mathrm{RG}}$ is the color index of the radio-selected galaxy. This criterion is the Butcher & Oemler (1984) definition of a blue galaxy transformed from the $B-V$ color index to $B-R$.

The result for the SBRGs and the HLRGs is seen in figure 5. This plot separates at zero the red population (<0) and the blue population (≥ 0). The color separation indicates that most of the luminous radio galaxies are probably red ellipticals, consistent with the well-known result that the host galaxies of luminous radio sources are ellipticals and powered by AGNs (**?**, *e.g.,*)]led95a. If we selected galaxies with a radio luminosity limit of $\leq 10^{23}$ W Hz^{-1}, we find that 39% (17/44) of these objects are blue, while the HLRG is only 4% (1/28) blue. However, if we restrict the upper radio luminosity of the galaxies to $10^{22.75}$ W Hz^{-1}, *i.e.,* the SBRG population, thereby statistically selecting mostly starburst galaxies, this results in 48% (15/31) of the galaxy population having colors that are bluer than Sab galaxies. Thus, by restricting the upper radio luminosity of the LLRGs to $10^{22.75}$ W Hz^{-1} we are thereby statistically selecting mostly starbursting galaxies, where the radio is powered by the ongoing SF. In the HLRG case, AGNs appear to be the power source for the radio emission. In Paper IV, we will spectroscopically classify the radio-selected objects thereby determining their dominant power source for the radio emission.

[4] Basically, the difference between the average $B-V$ color of a Sab galaxy and the average color of the red cluster sequence.

4.1.2. Absolute Magnitudes of Radio-selected Galaxies

Figure 6 shows the absolute magnitude distribution of the SBRG and the HLRG population. The SBRGs have an $\langle M_{\mathrm{R}}\rangle=-21.93\pm0.05$ while the HLRG have an $\langle M_{\mathrm{R}}\rangle=-22.33\pm0.07$ indicating that the SBRGs are less optically luminous than the HLRGs. Wilcoxon Rank test and the K-S test yield confidence levels >99.9% indicating that the SBRG and HLRG are from significantly different populations, based on the absolute magnitude distribution. These data suggest that the SBRG are probably spirals, while the high-luminosity radio sources are more likely to be massive cluster ellipticals.

4.2. Cluster Environment

What do these elevated f_{SBRG} values compared with the rest of the sample, tell us? Are they indicative of cluster environmental effects on galaxy evolution? If cluster environment is the cause of the radio enhancement, why do not all of our clusters have similar f_{SBRG} values? Since the SBRGs are more likely to be starburst galaxies, few rich cluster environments appear to stimulate massive SF in their galaxies. Since 'average' local galaxies generally do not experience radio emission at $\geq 10^{22.3}$ W Hz^{-1} without having vigorous amounts of SF (SFR $\gtrsim 5\,\mathrm{M}_\odot\,\mathrm{yr}^{-1}$) or possessing an AGN (Condon 1992), it may be that the environment in these few clusters is different and is somehow causing this radio weak galaxy population.

Both A1278 and A2125 have bi-modal X-ray and adaptively-smoothed optical number density distributions (**?**, see)]mor00, which is evidence for an ongoing cluster-cluster merger. Recent theoretical work by Bekki (1999) suggests that the rapidly varying gravitation potential of a group-cluster merger triggers a starburst in gas-rich galaxies. The triggering is done by exciting the non-axisymmetric structure of the galaxy, thereby funneling gas to the central region, commencing a starburst. Thus, cluster mergers may stimulate radio emission within gas-rich cluster members. However, other known group-cluster mergers in this sample, such as A168, A754, A2111, and A2256, do not show the same activity level in the radio ($\text{Ł}_{1.4\mathrm{GHz}}\geq 10^{22.3}$ W Hz^{-1}) as is seen in

A1278 and A2125. Tomita et al. (1996) looked for an enhanced blue fraction (f_B) in A168 but found none. One of their conclusions from this was that the cluster members are gas deficient, thus unable to support enhanced SFRs.

Another possible mechanism for the enhanced fraction of radio emitting galaxies in clusters is galaxy-galaxy interactions and/or mergers. In A2125, Ledlow et al. (1999) found that nearly 90% of both the red and blue radio-selected galaxies appeared in pairs ($< 30\,\mathrm{kpc}$ projected separation), compared with a pair fraction of ∼40% for other cluster galaxies. Spectroscopically-measured relative velocities indicate that only two of the 26 radio-selected galaxies (both starbursts) have $\Delta V \lesssim 300\,\mathrm{km\,s^{-1}}$. In those two cases, galaxy interactions are the likely trigger for the starburst. The other pairs are comprised of chance superposition of stars and galaxy pairs with $\Delta V \geq 500\,\mathrm{km\,s^{-1}}$. These high-speed galaxy encounters may support the galaxy harassment scenario (Moore et al. 1996).

As for A1689, it is a relaxed cluster whose fraction of SBRGs could not be enhanced by the cluster merger mechanism, but possibly enhanced by pressure confinement from its substantial intracluster medium (ICM). This also might be true for the high fraction of HLRGs found in A1689.

From Duc et al. (2002) mid-infrared ISOCAM[5] study of A1689 cluster core region, we find that out of the eleven radio-selected galaxies for this cluster, three are outside the ISOCAM field-of-view (fov). Of the remaining eight, three are not detected at 6.75μm ($LW2$ filter) and 15μm ($LW3$ filter), two are detected at 6.75μm but not at 15μm, while the final three are detected in both bands. Following the MIR classification criterion of Duc et al. (2002) we classify the radio galaxies as follows. For the three SBRGs in A1689 within ISOCAM's fov, one is not detected in either band, one is classified as a starburst, and the other as an AGN. For the five HLRGs within the ISOCAM's fov, all are classified as AGNs. However, the majority of the MIR galaxies detected by Duc et al. (2002) have $L_{1.4\,\mathrm{GHz}} < 2\times10^{22}\,\mathrm{W\,Hz^{-1}}$ indicating that any hidden star formation present in A1689 is below $5\,\mathrm{M_\odot\ yr^{-1}}$ ($\mathrm{M} \geq 5\mathrm{M_\odot}$).

[5]ISOCAM camera (Cesarsky et al. 1996) onboard the ISO satellite.

4.2.1. Cluster Parameters

Cluster Richness and Compactness

One important question is whether the richness (galaxy counts) $N_{2.0}$[6] of a cluster correlates with the fraction of radio galaxies. We did find a weak anti-correlation between f_{RG} and $N_{2.0}$ at the 90% confidence level, possibly suggesting that the detection rate for all radio galaxies does not scale with the number of galaxies surveyed. However, we found no significant ($\geq 2\sigma = 95\%$ confidence) correlation of f_{RG}, f_{SBRG}, or f_{SBRG} with richness ($N_{0.5}$ or $N_{2.0}$).

Another question is whether the compactness of a cluster is correlated to the radio galaxy fraction. Owen et al. (1999) discuss the radio population in A2125 and A2645, noting the excess of the SBRG population in irregular cluster A2125, with the lack of such a population in compact cluster A2645. Their result suggests that the large (21) SBRG population in A2125 may be driven by the ongoing cluster-cluster merger or the coalescence of multiple subunits (Wang et al. 1997). A2645 has the appearance of a relaxed, centrally-condensed compact cluster, whose population is dominated by red galaxies. Given that we have a mixture of cluster types (*e.g.,* regular and irregular) in our sample, we will try to decouple the population radio-selected galaxies from the cluster morphology by using the following compactness parameter.

Compactness parameter, defined as $\mathcal{C} = N_{0.5}/N_{2.0}$, is the ratio of the Bahcall (1981) counts, $N_{0.5}$, to the Abell et al. (1989), galaxy counts, $N_{2.0}$. This ratio provides a rough quantitative measure of a cluster's compactness or morphology (*i.e.,* regular-compact or irregular-open). We found no significant ($\geq 2\sigma = 95\%$ confidence) correlation for the whole sample between f_{RG}, f_{SBRG}, or f_{SBRG} with cluster compactness. This negative result might be due to projection effect on the sky where only well separated merging systems would have a large $\mathcal{C}$. Or possibly the rather brief ($\lesssim$0.3 Gyr) period that cluster-wide starburst phase could occur in such a cluster might have a large $\mathcal{C}$ but no large fraction of SBRG.

[6]$N_{2.0}$ represents the number of galaxies brighter than $M_{\mathrm{R}} = -20.5$ (roughly the number between $\mathrm{m_3}$ and $\mathrm{m_3}$+2.) within one Abell radius or 2.0 Mpc. See Morrison et al. (2003a) for details.

Cluster Blue Fraction

Morrison et al. (2003a) discusses our procedure for measuring $f_{\rm B}$. In brief, $f_{\rm B}$ is based on the Butcher & Oemler (1984) definition, with the exception that we use a fixed metric aperture of radius 0.5 Mpc centered on the X-ray peak of the cluster. The parameter $f_{\rm B}$ measures the blue galaxy population in the cluster core with respect to the cluster's red population, using a Sab galaxy as a fiducial point for defining the blue population. The K-correction and the color-magnitude effect have been applied to each cluster.

The $f_{\rm B}$ and f_{RG} values of the clusters are not correlated. This result is expected, given the different regions sampled. The parameter $f_{\rm B}$ is measured over the central core region of the cluster, whereas f_{RG} is measured over a much larger region, $r \leq 2.5$ Mpc, as discussed in the last section. In addition, the $f_{\rm B}$ magnitude limit is $R = -19$ compared to $R = -21$ for the radio-selected galaxies. Moreover, given the SFR threshold $\gtrsim 5\,{\rm M}_{\odot}\,{\rm yr}^{-1}$ that can be detected in the radio, typical late-type spiral galaxies (SFR$\lesssim 4\,{\rm M}_{\odot}\,{\rm yr}^{-1}$) that would be detected by the BO method would not be selected in the radio. However, the radio does detect dust-enshrouded starbursting galaxies that would not be selected by the BO method because of their rather red color.

X-ray Luminosity

The $f_{\rm RG}$ and $f_{\rm SBRG}$ values for all the clusters show no significant correlation with the X-ray luminosities of the clusters. Of interest is A2125 and A1278's $f_{\rm SBRG}$ values which have higher $f_{\rm SBRG}$ values at a similar X-ray luminosity. However, too few clusters exist with bimodal X-ray/optical distributions to draw any conclusions.

The high radio luminosity radio fraction ($f_{\rm HLRG}$) also fails to demonstrate any significant correlation with the $L_{\rm x}$ of the cluster. There is an indication that a pressure confinement enhancement effect may be taking place in A1689. This cluster has a high X-ray luminosity, as well as the highest $f_{\rm HLRG}$ fraction of any of the $z \lesssim 0.25$ clusters. While this is only one cluster, it does support the idea that pressure from the intracluster material could increase the radio luminosity of twin jets near the cluster center, where these HLRG sources are located.

5. Conclusion

In this paper we have studied the radio-selected galaxy population of a subsample of very rich ($R \geq 2$) Abell galaxy clusters with $z \leq 0.25$. The weak anti-correlation between $f_{\rm RG}$ and $N_{2.0}$ at the 90% confidence level suggests possibly that the detection rate for all radio galaxies does not scale with the number of galaxies surveyed. However, overall, we found no significant ($\geq 2\sigma = 95\%$ confidence) correlation or anti-correlation of $f_{\rm RG}$, $f_{\rm SBRG}$, or $f_{\rm SBRG}$ with cluster richness ($N_{2.0}$ or $N_{0.5}$), compactness, blue fraction, or x-ray.

There are only a few clusters that have radio galaxy fractions (SBRG and HLRG) that are inconsistent with the rest of the sample. We find the following average radio galaxy fractions: $\langle f_{\rm SBRG} \rangle = 0.022 \pm 0.003$ and $\langle f_{\rm HLRG} \rangle = 0.024 \pm 0.003$. The cluster with an excess at the $>$ 99.99% confidence level of SBRGs is A2125, with a $f_{\rm SBRG} = 0.09 \pm 0.03$. This is *not* a richness-induced effect as we normalized by the number of galaxies sampled. Two clusters with weak $\sim$ 90% confidence level deviations from $\langle f_{\rm SBRG} \rangle$ are A1278 at 0.05 ± 0.03 and A1689, at 0.05 ± 0.03.

The bimodal structure in the optical and X-ray for A1278 and A2125 suggests that a possible cluster-cluster merger may be driving this excess in SBRGs. The mechanism for the increased fraction of SBRGs in A1689 may be the result of the ISM of the galaxies being compressed by their passage through the ICM. All the SBRGs in A1689 are within a projected distance of 0.8 Mpc from cluster core.

The large fraction of HLRGs in A1689 (0.09 ± 0.04) and A1940 (0.06 ± 0.03) may also be a result of the cluster environment. The HLRGs close projected distance from the cluster center ($<$ 0.8Mpc for both clusters) suggests that this population may be enhanced due to pressure confinement by the ICM. The MIR ISOCAM results for A1689's radio galaxy population suggest most are AGN in nature lends support to this idea.

The different spatial distribution between the SBRGs and the HLRGs is one of the most significant results of this paper. The core radius values of the SBRGs is $r_{\rm c} = 0.40 \pm 0.08$ Mpc. These are a factor $> 3\times$ larger than the average value of

$r_c = 0.12 \pm 0.02$ Mpc for HLRGs. The large difference in the fitted core radii values of the SBRGs and the HLRGs indicates a strong difference exists between their representative populations. The HLRGs are probably a subclass of the cluster's massive *red* elliptical population, while the SBRGs have a distribution more like the *blue* spiral population.

The difference in $\langle M_R \rangle$ values between the SBRGs and the HLRGs indicates an absolute magnitude segregation between the two populations, with the higher optical luminosity galaxies belonging to the HLRGs. This is in agreement with the core radius results for the SBRGs and HLRGs. Also the colors of the three radio populations suggest that the SBRGs have colors that are much bluer than the HLRGs. These results indicate that a large fraction of the SBRGs are probably gas-rich disk galaxies with SFR $\gtrsim 5\,\mathrm{M_\odot\,yr^{-1}}$. It is unclear as to what triggered the SF in the SBRGs for most clusters. It must be noted that contamination due to AGNs in the SBRGs has not been completely removed. Paper IV will cover the spectroscopic classifications of the radio-selected galaxies.

A larger, more morphologically diverse sample is currently being studied that contains more irregular rich clusters similar to A1278 and A2125. This will allow us to decouple the effects that cluster dynamics have on the radio properties of cluster galaxies.

We thank an anonymous referee for helpful comments. We would also like to thank Carol Lonsdale, Neal Miller, Michael Ledlow, Bill Keel, and Schuyler Van Dyk. G.E.M. acknowledges financial support from the NRAO predoctoral fellowship program during which most of this work was completed. G.E.M. also gratefully acknowledges the support of NASA-JPL (contract #1147-001 and #1166) and also the support of Vanguard Research, Inc.

REFERENCES

Abell, G. O., Corwin, H. G., J., & Olowin, R. P. 1989, ApJS, 70, 1

Adami, C., Mazure, A., Katgert, P., & Biviano, A. 1998, A&A, 336, 63

Bahcall, N. A. 1975, ApJ, 198, 249

—. 1981, ApJ, 247, 787

Balland, C., Silk, J., & Schaeffer, R. 1998, ApJ, 497, 541

Bekki, K. 1999, ApJ, 510, L15

Butcher, H. & Oemler, A., J. 1984, ApJ, 285, 426

Caldwell, N. & Rose, J. A. 1997, AJ, 113, 492

Cesarsky, C. J., Abergel, A., Agnese, P., et al., 1996, A&A, 315, L32

Condon, J. J. 1989, ApJ, 338, 13

—. 1992, ARA&A, 30, 575

Condon, J. J., Anderson, M. L., & Helou, G. 1991, ApJ, 376, 95

Duc, P.-A., Poggianti, B. M., Fadda, D. and Elbaz, D., Flores, H., Chanial, P., Franceschini, A., Moorwood, A., & Cesarsky, C.2002, A&A, 382, 60

Dwarakanath, K. S. & Owen, F. N. 1999, AJ, 118, 625

Evrard, A. E. 1989, in Clusters of Galaxies, ed. W. R. Oegerle, M. J. Fitchett, & L. Danly (Cambridge: Cambridge Univ. Press), 287

Geller, M. J. & Beers, T. C. 1982, PASP, 94, 421

Girardi, M., Biviano, A., Giuricin, G., Mardirossian, F., & Mezzetti, M. 1995, ApJ, 438, 527

Kennicutt, R. C., Schweizer, F. & Barnes, J. E. 1998, in Saas-Fee Advanced Course 26: Galaxies: Interactions and Induced Star Formation, 26

King, I. 1962, AJ, 67, 471

Lacey, C. & Cole, S. 1993, MNRAS, 262, 627

—. 1994, MNRAS, 271, 676

Ledlow, M. J. & Owen, F. N. 1995a, AJ, 110, 1959

—. 1995b, AJ, 109, 853

Ledlow, M. J., Owen, F. N., Dwarakanath, K. S., Keel, W. C., & Morrison, G. E. 1999, in ASP Conf. Ser. 176: Observational Cosmology: The Development of Galaxy Systems, 83

Moore, B., Katz, N., Lake, G., Dressler, A., & Oemler, A., J. 1996, Nature, 379, 613

Morrison, G. E., Owen, F. N., & Ledlow, M. J. 2003a, paper III, in preparation

Morrison, G. E., Owen, F. N., Ledlow, M. J., Hill, J., & Herter, T. 2003b, paper IV, in preparation

Morrison, G. E., Owen, F. N., Ledlow, M. J., Keel, W. C., Hill, J. M., & Voges, W. 2002, paper I, accepted by ApJS

Oemler, A., J. 1974, ApJ, 194, 1

Oemler, Augustus, J., Dressler, A., & Butcher, H. R. 1997, ApJ, 474, 561

Owen, F. N., Keel, W., Ledlow, M. J., & Morrison, G. E. 1999, AJ, 118, 633

Sarazin, C. L. & Quintana, H. 1985, Galaxy Distribution in Abell Clusters (University of Virginia report)

Stanford, S. A., Eisenhardt, P. R. & Dickinson, M. 1998, ApJ, 492, 461

Tomita, A., Nakamura, F. E., Takata, T., Nakanishi, K., Takeuchi, T., Ohta, K., & Yamada, T. 1996, AJ, 111, 42

Wang, Q. D., Ulmer, M. P., & Lavery, R. J. 1997, MNRAS, 288, 702

West, M. J. & Bothun, G. D. 1990, ApJ, 350, 36

White, S. D. M. 1976, MNRAS, 177, 717

AAS LaTeX macros v5.0.

Table 1

Radio Selected Galaxy Classes at 1.4 GHz

Class	$\log(L_{\rm min})$ W Hz^{-1}	$\log(L_{\rm max})$ W Hz^{-1}
SBRG	22.3	22.75
LLRG	22.3	23
HLRG	23	25

FIGURE CAPTIONS

Fig. 1.— Projected surface density distribution of radio-selected galaxies. Solid line: SBRGs. Dotted line: HLRGs.

Fig. 2.— Projected surface density distribution of high-luminosity radio-selected galaxies versus the projected radial distance from cluster center. The curve is a King model, indicating an excess of galaxies at the center of the cluster. The error bars are Poisson errors based on the number counts within each bin.

Fig. 3.— Same as in Fig. 2 but for the SBRGs. The King model here, indicates an excess of galaxies beyond $r \gtrsim 0.2\,\mathrm{Mpc}$. The error bars are Poisson errors based on the number counts within each bin.

Fig. 4.— The SBRGs radio galaxy fractions are represented by the solid line. A2125 is an outlier at 0.09. The HLRGs radio galaxy fractions are shown by the hatch patter . A1689 is an outlier at 0.09 which over lies A2125 data point.

Fig. 5.— Histogram of Butcher-Oemler defined blue (≥ 0) and red (< 0) radio galaxies. Solid line: SBRG. Dashed line: HLRGS.

Fig. 6.— SBRG (solid line) and HLRG (dashed line) absolute magnitudes.

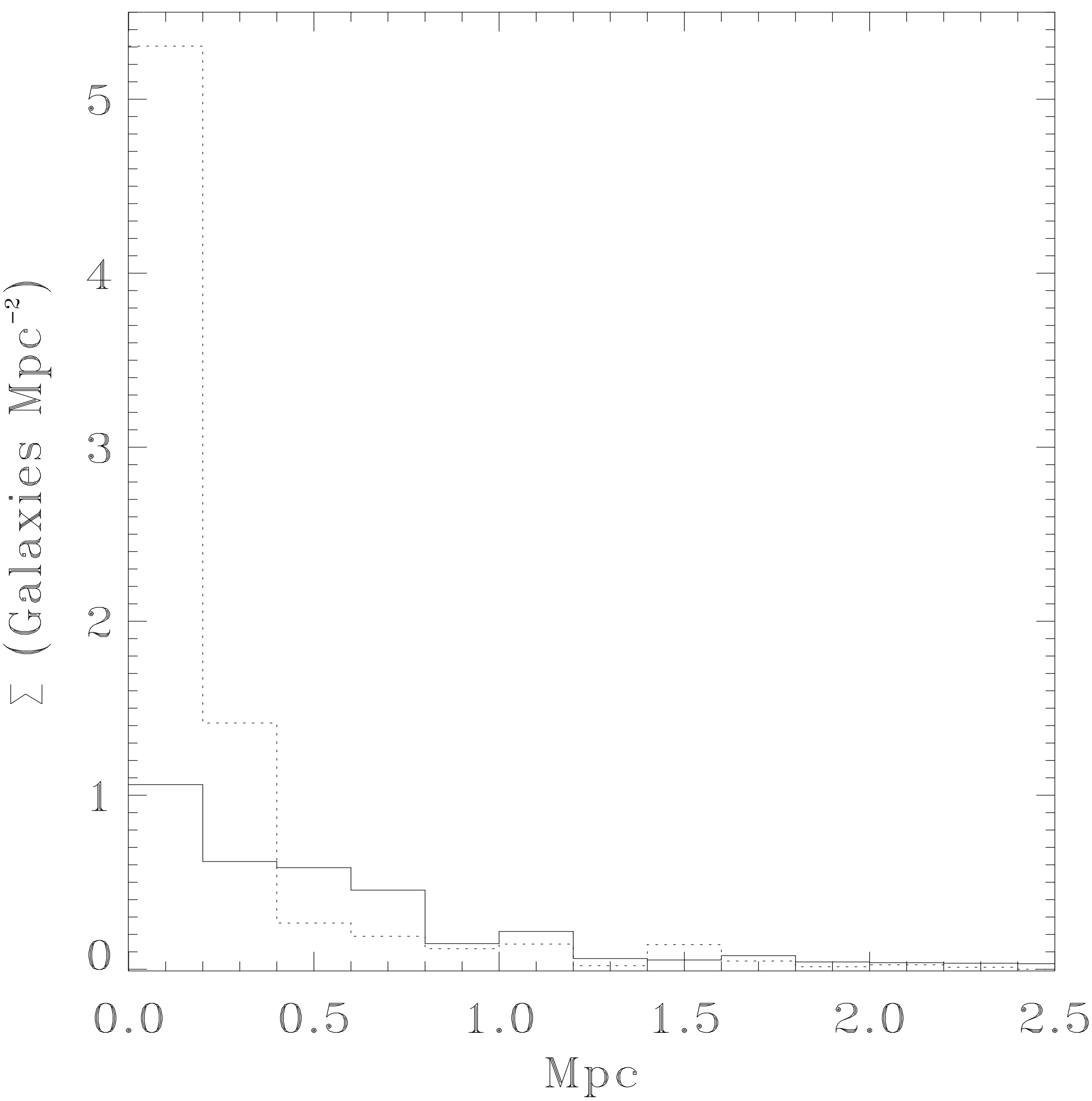

5
4
3
2
1
0
Σ (Galaxies Mpc⁻²)
0.0
0.5
1.0
1.5
2.0
2.5
Mpc

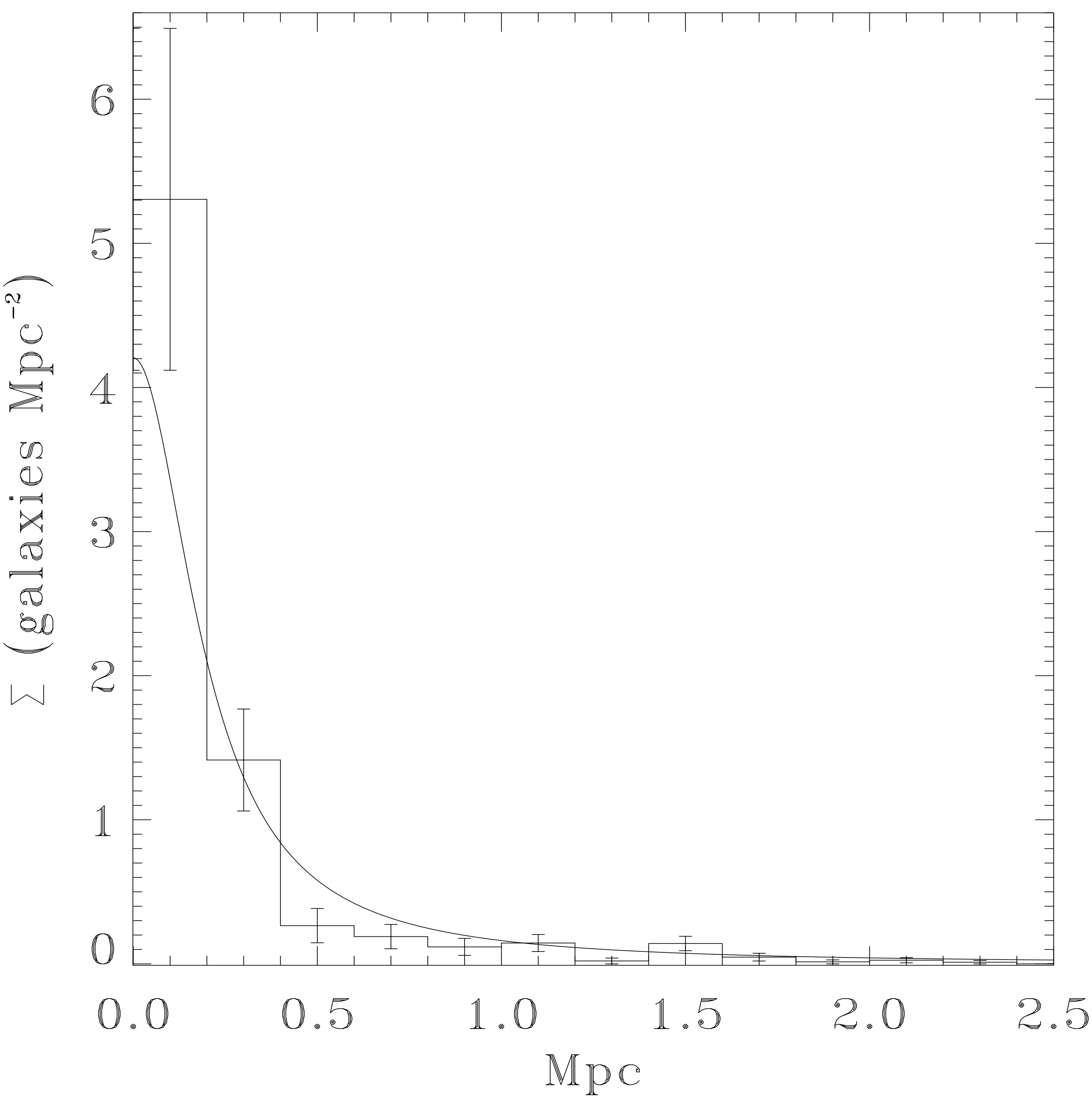

Σ (galaxies Mpc⁻²)
Mpc
0
1
2
3
4
5
6
0.0
0.5
1.0
1.5
2.0
2.5

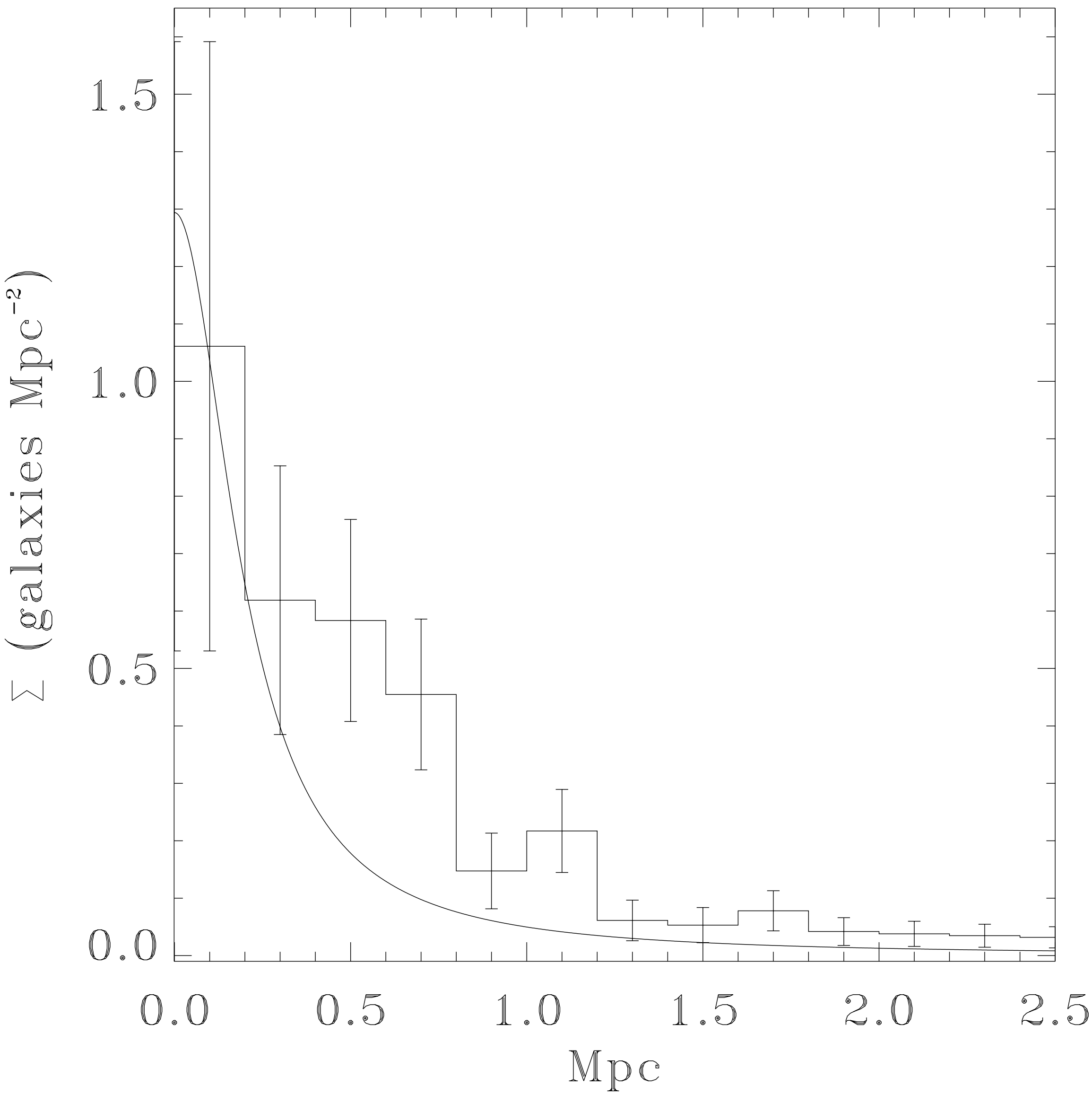

1.5
1.0
0.5
0.0
0.0
0.5
1.0
1.5
2.0
2.5
Mpc
Σ (galaxies Mpc^{-2})

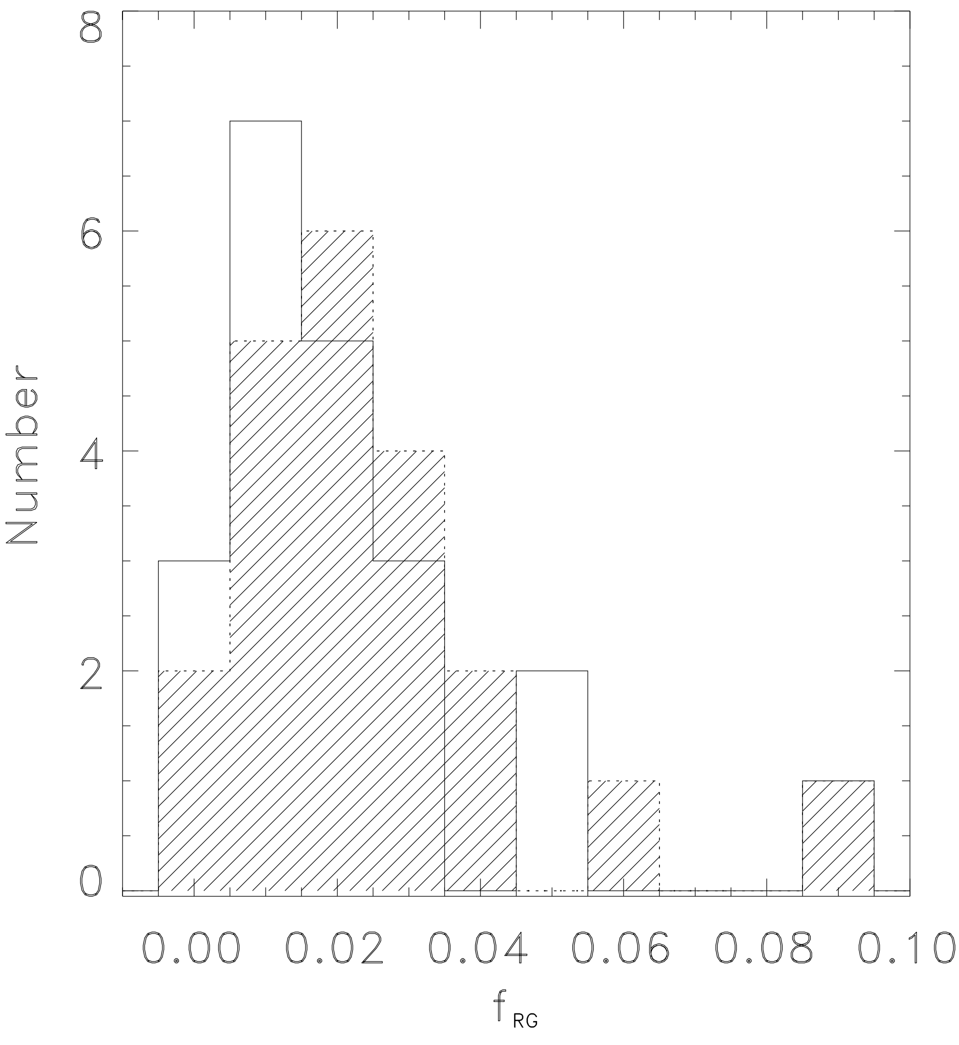

Number
8
6
4
2
0
0.00
0.02
0.04
0.06
0.08
0.10
f RG

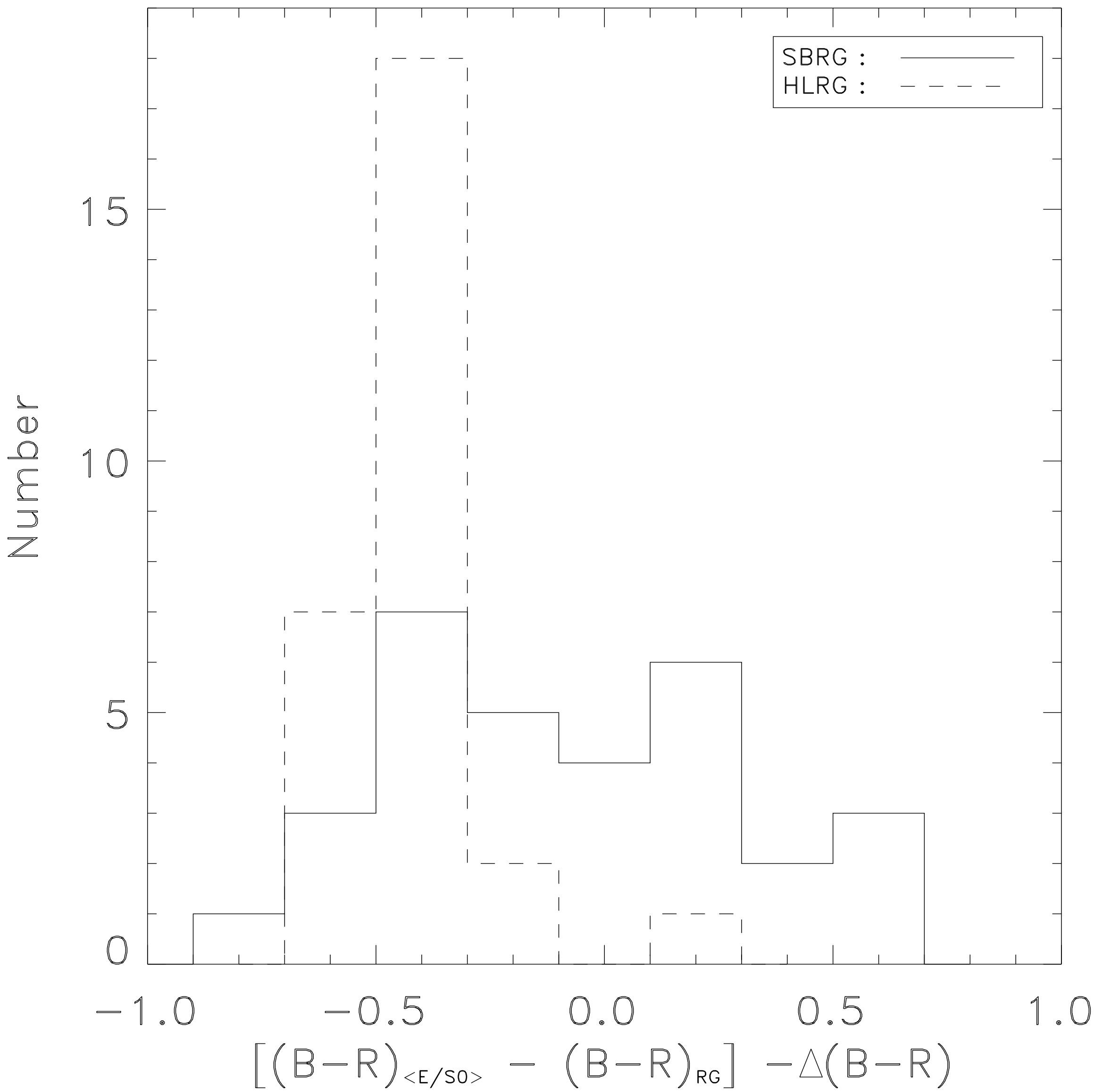

SBRG :
HLRG :
Number
15
10
5
0
−1.0
−0.5
0.0
0.5
1.0
$[(B-R)_{<E/S0>} - (B-R)_{RG}] - \Delta(B-R)$

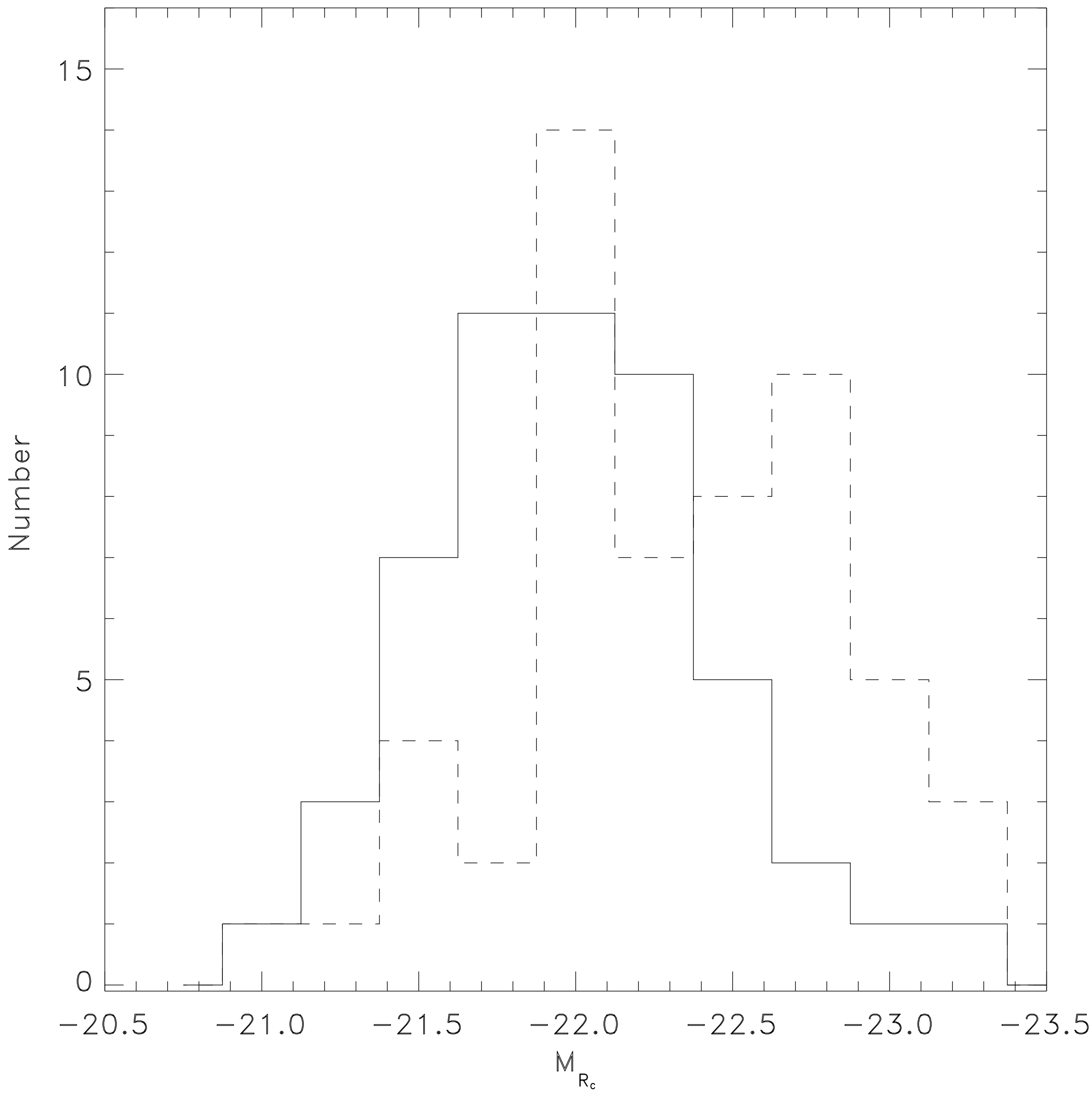
15
10
5
0
Number
−20.5
−21.0
−21.5
−22.0
−22.5
−23.0
−23.5
M_{R_c}